Dynamic Primitives Limit Human Force Regulation During Motion

A. Michael West Jr. ⓘ, *Graduate Student Member, IEEE*, James Hermus ⓘ, Meghan E. Huber ⓘ, *Member, IEEE*, Pauline Maurice ⓘ, *Associate Member, IEEE*, Dagmar Sternad ⓘ, *Member, IEEE*, and Neville Hogan ⓘ, *Member, IEEE*

Abstract—Humans excel at physical interaction despite long feedback delays and low-bandwidth actuators. Yet little is known about how humans manage physical interaction. A quantitative understanding of how they do is critical for designing machines that can safely and effectively interact with humans, e.g. amputation prostheses, assistive exoskeletons, therapeutic rehabilitation robots, and physical human-robot collaboration. To facilitate applications, this understanding should be in the form of a simple mathematical model that not only describes humans' capabilities but also their limitations. In robotics, hybrid control allows simultaneous, independent control of both motion and force and it is often assumed that humans can modulate force independent of motion as well. This letter experimentally tested that assumption. Participants were asked to apply a constant 5 N force on a robot manipulandum that moved along an elliptical path. After initial improvement, force errors quickly plateaued, despite practice and visual feedback. Within-trial analyses revealed that force errors varied with position on the ellipse, rejecting the hypothesis that humans have independent control of force and motion. The findings are consistent with a feed-forward motion command composed of two primitive oscillations acting through mechanical impedance to evoke force.

Index Terms—Physical human-robot interaction, compliance and impedance control, force control.

I. INTRODUCTION

THE majority of human neuro-motor control research to date has focused on the control of motion during free unconstrained reaching without physical contact (for review see [1], [2]). In this case, relating a planned motion to an actual motion is sufficient to describe the control system. In robotics, the mathematics underlying motion control is well understood [3]. However, most tasks that humans and robots perform require physical interaction with the external environment; for such interactive tasks, motion control alone is insufficient.

During physical interaction, bidirectional forces between the actor and the environment critically affect the behavior of the coupled system. If humans regulate motion during free reaching, a simple extension of this idea to contact tasks may be to regulate both force and motion. In robotics, hybrid control allows for simultaneous and independent control of both motion and force in complementary subsets of the workspace [4], [5]. In human motor control, it is yet unresolved whether humans can control force independent of motion.

Several studies in human motor neuroscience have reported findings in support of such hybrid control. For example, Chib *et al.* [6] found that hybrid motion/force control can describe how humans performed an interaction task in a virtual force field. Casadio *et al.* [7] presented and experimentally validated a computational model of how the neural system may combine two independent modules that separately control motion and force. Further, neural activity in the motor and parietal cortex of non-human primates indicate that there are separate modules for the control of force and motion [8]–[10].

On the other hand, it has been shown that the central nervous system (CNS) contains a controller that modulates the coupling of force and motion [11], [12]. Other studies demonstrated that humans modulate the relation between motion and force during upper limb reaching in unstable force fields [13]–[16]. Additionally, our own previous research showed that exerted force depended on the velocity profile when grasping and following a robot manipulandum. Specifically, participants were asked to trace the motion of a robot manipulandum without exerting force as it moved on an elliptical path with varying velocity profiles [17]. If force can be controlled independent of motion, the velocity profile should not matter; however, it did.

This study aimed to examine human control of physical interaction that could resolve these seemingly contradictory results.
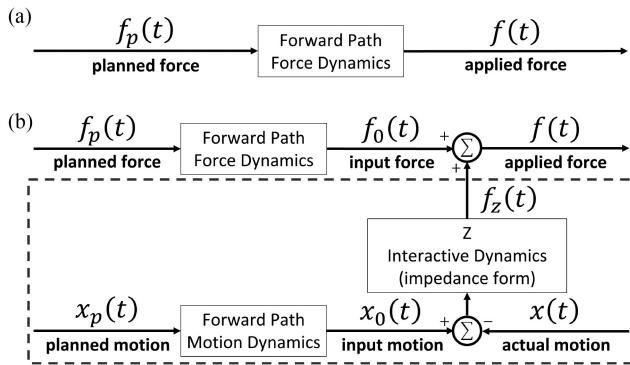
Fig. 1. **(a) Direct force control.** Applied force is a function of a planned force that is independent of motion. **(b) Indirect force control.** Applied force is a function of a planned force but also depends on motion. Further details are in the Discussion section.

We conducted an experiment in which participants physically interacted with a motion-controlled robot to test whether humans could regulate force independent of motion. We refer to this independent control as "direct force control" (Fig. 1 a). Explicitly, direct force control applies an actual force as a function of only a planned force. This function is an operator that may be dynamic and nonlinear. If participants can regulate force independent of motion, direct force control can be accepted as a plausible schema for human physical interaction. Conversely, if humans are unable to decouple force from motion, an alternative hypothesis is "indirect force control". With indirect force control, a planned force $f_p(t)$ may still exist in the forward path, but an impedance term $Z\{\cdot\}$ is needed to relate the difference between input motion $x_0(t)$ and actual motion $x(t)$ to the output force $f(t)$ (Fig. 1 b). The core feature of indirect force control is that force depends on motion.

The direct force control hypothesis leads to a testable prediction: Errors in contact force will be independent of motion. Thus in this experiment, participants were instructed to apply a specific constant force on a robot manipulandum in its direction of motion as it moved along an elliptical path. To give participants the best opportunity to complete the task, the robot moved with a velocity profile that matched human movement preferences, i.e., angular velocity scaled with curvature with a power of 2/3 [17], [18]. Despite visual feedback and some practice, errors in exerted force persisted and were dependent on motion, suggesting (1) a coupling of force and motion, and (2) the existence of an underlying structure in the feedforward motion planning signal. Additional analysis of previous data from [17] further validated the current results. In sum, this work showed that interactive dynamics are significant and of particular concern in (1) quantification of human performance and in (2) physical human-robot interaction.

II. METHODS

A. Participants

Eleven healthy right-handed individuals (3 females, 8 males; ages from 19 to 35 years old) participated in the experiment for some compensation. All participants signed a consent form
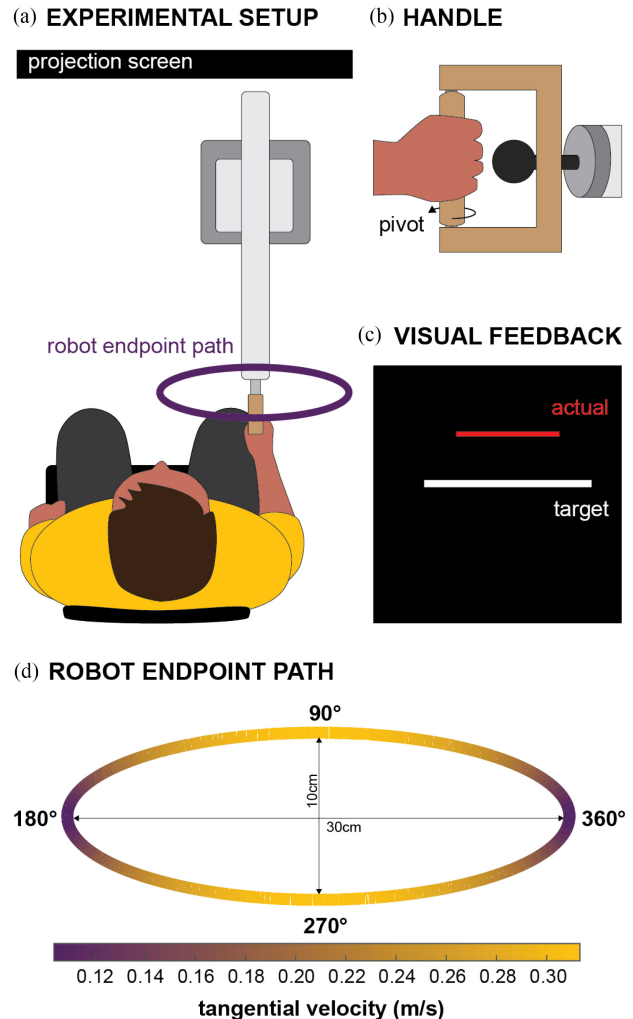
Fig. 2. **Experimental setup. (a)** Top-down view of the experimental setup. Participants were instructed to hold the handle of a moving robotic manipulandum and apply a constant force in the direction of the robot's motion. The elliptical path of the robot endpoint is displayed on the figure for clarity. However, participants did not see any visual display of the robot path. **(b)** Robot handle used to decouple human wrist and robot end-effector orientations. **(c)** To provide visual feedback, the projection screen displayed a stationary white bar indicating the target tangential force of 5 N and a moving red bar indicating the current applied tangential force. Visual feedback was given during Block 1 V and Block 2 V. Otherwise, the screen was black. **(d)** Elliptical trajectory of the robot endpoint (i.e., handle) in the horizontal plane. The robot manipulandum moved counterclockwise and followed a velocity profile that was in accordance with the two-thirds power law [18]. Tangential velocity is shown by color.

which explained the experiments' procedures. The experimental protocol was approved by the Institutional Review Boards of Northeastern University and the Massachusetts Institute of Technology.

B. Experimental Procedures

1) Task and Instructions: Participants were instructed to hold the handle of a moving robotic manipulandum (HapticMaster) [19] and apply a constant 5 N force in the direction of robot motion (i.e., tangential direction) as it traversed an elliptical trajectory in a horizontal plane (Fig. 2 a).

Participants performed the experiment seated and held the robot through a vertical handle which could pivot around its vertical axis; the pivot decoupled the robot end-effector orientation and the participant's wrist orientation (Fig. 2 b). Participants were positioned such that when holding the robot handle at the 270° position of the ellipse (Fig. 2 d), the right upper arm hung downward slightly away from the torso. This position aligned the forearm with the minor axis of the ellipse. The robot height was adjusted such that the forearm was approximately parallel to the ground. This resulted in an angle between the upper arm and forearm of approximately 90° (Fig. 2 a-b).

2) Visual Display: Participants sat approximately 2.2 m in front of a projection screen (height: 1.8 m, width: 2.4 m). In conditions with visual feedback, two horizontal bars appeared on the screen (Fig. 2 c). A red horizontal bar moved vertically to indicate the tangential force (averaged over 80 ms) applied by the participant onto the robot; the stationary white bar indicated the desired tangential force of 5 N. Otherwise, the screen was black.

3) Control of Robot Motion: The robot handle was commanded to move counterclockwise along an elliptical path (major axis = 30 cm, minor axis = 10 cm) on a horizontal plane with a period of 3 s (Fig. 2 d). The velocity profile of the robot handle followed the so-called 2/3 power-law relation [17], [18] between path curvature and angular velocity (Fig. 2 d), decreasing in highly curved portions and increasing in less curved portions. The position of the robot handle was controlled with a Cartesian PD controller; a high proportional gain was used such that deviation from the desired trajectory was negligible. The desired position of the robot was updated at 700 Hz, and an internal force control loop ran at 2 kHz.

C. Experimental Design

To assess the effect of practice and visual feedback on force control, participants performed four experimental blocks; each block consisted of 15 trials. In each trial, the robot continuously traversed the elliptical path four times with a period of 3 s per cycle; each trial lasted 12 s. Blocks 1V and 2V presented visual feedback as shown in Fig. 2 c. Blocks 1NV and 2NV did not present visual feedback. Participants always performed the four blocks in the following order: 1V, 1NV, 2V, 2NV. In all four blocks, participants were instructed to maintain a constant force of 5 N in the tangential direction. At the start of each trial, participants heard three short beeps through a headset, after which the robot began to move. Between blocks, participants were allowed to take a break if needed.

A familiarization block, referred to as Block F, preceded the four experimental blocks. It also consisted of 15 trials of 12 s each. There, participants were instructed to maintain a constant level of force in the tangential direction of the robot motion. The exact level of force applied was not specified and there was no visual feedback. After Block F, participants were given 60 s to familiarize themselves with the visual feedback. During that time, the robot was in a stationary position and participants could apply forces against the robot. In total, the experiment lasted just over an hour.

D. Dependent Measures and Data Processing

The force that participants applied to the robot handle was measured at ~560 Hz with a 3 DoF force sensor mounted at the robot end effector. In each trial, the tangential component of the force applied by the human to the robot was calculated and resampled as a function of robot position along the elliptical path at a resolution of 1°.

Angular position along the elliptical path was defined using the eccentric anomaly,[1] E, such that $E = atan(ay/bx)$, where a and b were half the length of the major and minor axes of the ellipse, respectively. x and y were the magnitudes of the position vector in the direction of the major and minor axes in Cartesian space, respectively.

For each trial, task performance was summarized by calculating the root-mean-square (RMS) of force error. Force error was defined as the difference between the actual tangential force and the target tangential force of 5 N. The tangential force was resampled as a function of robot position along the elliptical path at a resolution of 1°. To avoid the potential influence of transient behavior, the first cycle of each trial was omitted in the calculation of the RMS error.

E. Data Analysis and Statistics

All data were processed and statistical analyses were performed using custom scripts in MATLAB. The significance level for statistical tests was $\alpha = 0.05$. Unless stated otherwise, only data from the four experimental blocks (i.e., Blocks 1V, 1NV, 2V, and 2NV) were included in the statistical analyses.

1) Performance Improvements: Prior to testing the effects of practice and feedback in the four blocks, performance improvements were assessed within blocks across trials by calculating linear regressions between RMS force error and trial number. Performance improvement was indicated if the slope was different from zero, i.e., the 95% confidence interval of the slopes did not include zero.

To determine where participants' performance reached steady state, the regression slopes between trial number and the average RMS force error across participants were calculated iteratively for the last 15, 14, 13, trials and so forth until an insignificant slope was found. This occurred when the linear regression was computed over the last 9 trials (i.e. from trial 7 to 15). The lack of a significant slope with the RMS of force error and trial number justified averaging measures over the last 9 trials within a block.

To assess whether visual feedback or practice across the 2 blocks influenced performance, the block means of all participants were calculated over the steady state portion of each block. These block means of RMS force error were submitted to a 2 (block) x 2 (feedback) repeated-measures ANOVA.

2) Existence of Motion-Dependent Force Errors: To assess the presence of motion-dependent patterns in the force error, the auto-correlation function of force error (as a function of robot angular position) was calculated for each trial. The lag

---

[1]The eccentric anomaly is one of three angles (or "anomalies") identified by Johannes Kepler in his study of celestial mechanics to describe the position of a body that is moving along an elliptical orbit [20]. The other two angles are the true anomaly and the mean anomaly.
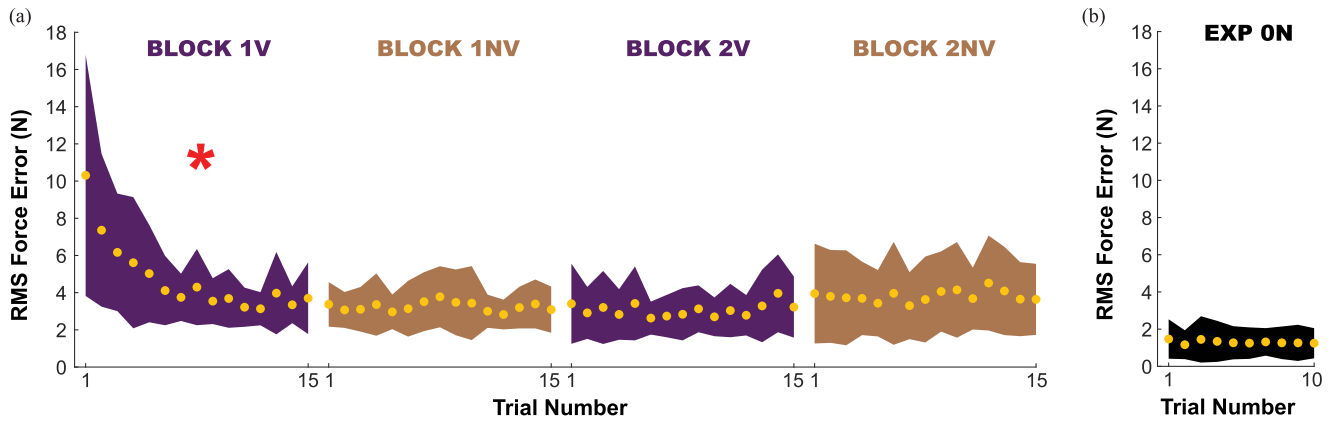
Fig. 3. **Mean RMS of force error across participants in each trial for (a) all experimental blocks in the main experiment, and (b) Experiment 0 N.** Yellow dots depict the average value across participants. The shaded region depicts ± 1 standard deviation across participants. An asterisk (*) indicates a significant linear relation between the mean RMS force error and trial number calculated across participants for each block.

with the maximum peak in the auto-correlation function (hereafter referred to as maximum lag) and its corresponding auto-correlation coefficient (maximum auto-correlation coefficient) were identified.

Two clusters were identified in the distribution of lags at maximum auto-correlation and their means were determined. Trials where the maximum auto-correlation coefficient was less than 0.1 were omitted from the analysis of position dependency of force error (4 out of 825 trials). From visual inspection, these low maximum auto-correlation coefficient values resulted from isolated uncharacteristic changes in RMS force error during the trial. They also occurred at lag values that were significant outliers.

III. RESULTS

A. Performance Improvements

1) Change in RMS Force Error Within Blocks: Inspection of the grouped time series of force error revealed that subjects showed a consistent decline of the force error in the first part of Block 1V (Fig. 3 a). The iteratively computed linear regressions between the average RMS force error across participants and trial for the last 15, 14, 13, and so forth trials identified that the force error values in Block 1V plateaued when calculated over the last 9 trials (i.e., from trial 7 to 15). From trial 7 onwards the regression slopes did not differ from zero. As this initial drop of error seemed to be a result of familiarization, subsequent analyses only examined the last 9 trials of all four blocks to evaluate the errors reached in each condition.

2) Effect of Practice and Visual Feedback on RMS Force Error Across Blocks: To statistically evaluate whether visual feedback and practice had a significant effect on the force error, a 2 (block) x 2 (feedback) repeated-measures ANOVA was conducted. The force error revealed a significant interaction ($F_{1,10} = 15.74, p = 2.66e - 03$) as the mean RMS error decreased from Block 1V ($M = 3.63N, SD = 1.12N$) to Block 1NV ($M = 3.30N, SD = 1.12N$) and increased from Block 2V ($M = 3.08N, SD = 1.32N$) to Block 2NV ($M = 3.86N, SD = 1.96N$) (Fig. 4 a). However, neither the main effect of block (p = 0.99), nor the main effect of feedback (p =
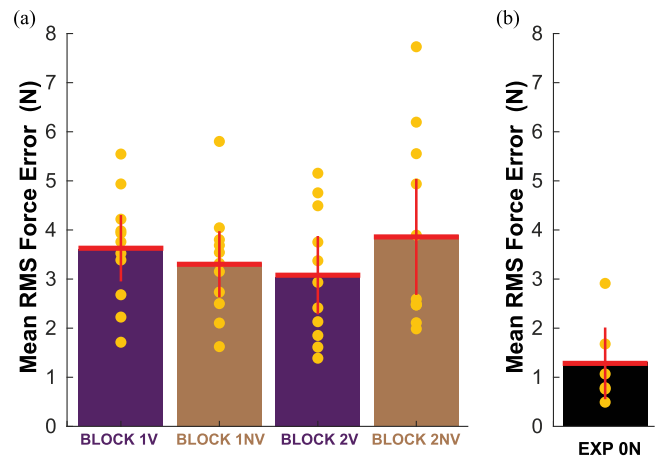

Fig. 4. **Mean RMS of force error from the last 9 trials for (a) all experimental blocks in the main experiment, and (b) Experiment 0 N.** Yellow dots depict individual participants. Error bars depict ± 2 standard errors of the mean. The mean RMS of force error was significantly higher in all experimental blocks of the main experiment compared to Experiment 0 N (Table I).

0.60) were statistically significant. Recall, all subjects completed the experiment in order: Block 1V, 1NV, 2V, 2NV. Thus, the increase in mean RMS of force in Block 2 was likely the result of cognitive or physical fatigue as the experiment was quite long.

B. Existence of Motion-Dependent Force Errors

Given this indifference to feedback and practice, the time series of force error were inspected. As illustrated by the raw force data shown for a representative participant in Fig. 5, force error was periodic with pronounced peaks at multiples of $180°$ in all blocks. The means of each cluster identified in the maximum lag data of trials in Blocks 1V, 1NV, 2V, and 2NV were $179.3°$ and $359.3°$ (Fig. 6 a). The average maximum auto-correlation coefficient was 0.43 ($SD = 0.13$). Trials with maximum lags of $360°$ indicate that the peaks in force error at half and full cycle were different, while the maximum lag at $180°$ indicates that the two peaks in force error were similar. Analyses of individual participants revealed that five subjects showed higher force applied at $180°$ and six subjects showed higher force applied
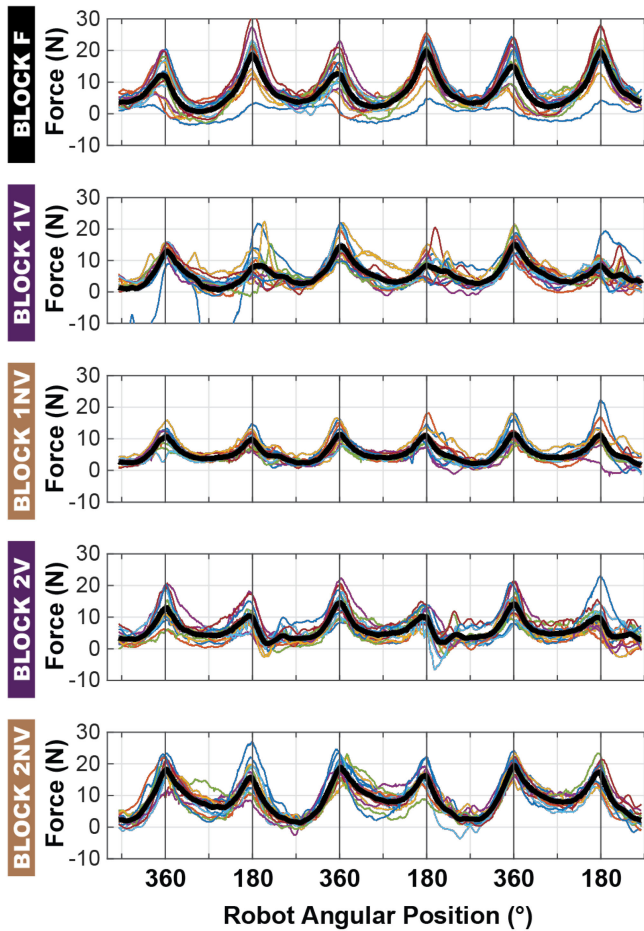
Fig. 5. **Raw force data in each block for a representative participant.** For each of the 5 blocks in the main experiment, plots of tangential force over robot angular position are shown for the last 3 cycles of every trial. The tangential force was resampled as a function of robot position along the elliptical path at a resolution of $1°$. Each trial is depicted with a thin, colored line, and the average across all trials is depicted with a thick, black line.

Fig. 6. **Evidence of motion-dependent periodic force errors for all trials in (a) Blocks 1V, 1NV, 2V, and 2NV of the main experiment, (b) Block F of the main experiment (c) Experiment 0N.** Histogram of lags of maximum autocorrelation (referred to as maximum lag) values measured in units of robot angular position. In all conditions, two clusters were identified. The solid lines indicate the mean of each cluster, and the dashed lines depict ± 1 standard deviation of each cluster.

at $360°$. Taken together, these results indicate that force error strongly depended on the phase of the oscillatory robot motion.

Given this pronounced periodicity in the experimental blocks that specified 5 N force, we also examined whether this periodicity was present spontaneously. The same autocorrelation analyses were run on the trials of the familiarization block (Block F). Fig. 6 b shows two clusters with mean values of $179.9°$ and $359.5°$. The average maximum auto-correlation coefficient was 0.53 ($SD = 0.12$). As illustrated in Fig. 6 b, these results give strong evidence for a spontaneous coupling of motion and force.

IV. ADDITIONAL RESULTS

To further validate the existence of motion-dependent force errors, similar analyses were performed on data collected in a previously published study of human-robot interaction by Maurice *et al.* (see [17] for full experimental details). The objective of that study was to examine how humans adapt to different velocity patterns in elliptic planar robot movements, identical to the ones used in this study. However, instead of being instructed to apply a constant 5 N force in the tangential direction, participants were instructed to minimize the total force magnitude applied to

the robot end effector (i.e., apply 0 N total force). Participants ($N = 6$) performed 10 trials, where each trial consisted of 4 cycles as in the present study. No visual feedback was provided to participants at any point in the experiment. This dataset is referred to as Experiment 0 N.

To allow comparison with the results of the main experiment, force error was defined as the difference between the actual tangential force and the target tangential force of 0 N. Otherwise, all data processing methods and dependent measures were identical.

A. Performance Improvements

The linear regression between the average RMS force error calculated across participants and trial numbers was not statistically significant, indicating no evidence of change in task performance with practice (Fig. 3 b).

B. Existence of Motion-Dependent Force Errors

Two clusters were identified in the maximum lag data. The means of each cluster were $173.5°$ and $359.8°$ (Fig. 6 c), and the

TABLE I
STATISTICAL RESULTS COMPARING MEAN RMS OF FORCE ERROR BETWEEN MAIN EXPERIMENT AND EXPERIMENT 0 N

	t statistic (df = 15)	p value
Block 1V - Experiment 0N	4.40	$5.21e-04$
Block 1NV - Experiment 0N	3.79	$1.77e-03$
Block 2V - Experiment 0N	2.95	$9.87e-03$
Block 2NV - Experiment 0N	2.02	$8.62e-03$

average maximum auto-correlation coefficient was 0.41 ($SD = 0.11$). Despite the difference in task instruction, these results were strikingly similar to those in the main experiment. Most importantly, they indicate that the force errors were also motion-dependent.

C. Differences in Force Error Magnitude

While the force patterns were dependent on motion in both experiments, the magnitude of the force errors differed. Independent t-tests compared the mean RMS force errors from each block of the main experiment with those of Experiment 0 N. Note that in all cases, the mean RMS force error was calculated over the last 9 trials for consistency. As summarized in Table I and depicted in Fig. 4 a-b, the mean RMS force error was significantly higher in all blocks of the main experiment (Bonferroni adjusted $\alpha = 0.05/4 = 0.0125$). Despite more practice and added visual feedback, participants who aimed to apply 5 N force on the moving robot performed considerably worse than those instructed to minimize total force applied.

V. DISCUSSION

This work investigated humans' ability to directly modulate force during motion. Subjects were asked to apply a constant force on a robot manipulandum moving along an elliptical path. The hypothesis of direct force control predicted that errors in contact force would be independent of motion. Here, the force errors observed throughout the entire main experiment depended on motion. Force error showed a periodic pattern consistent with the periodicity of the path; it varied with motion. After initial performance improvements, participants did not reduce force errors with practice, even when visual feedback was provided. Motion-dependent patterns in force error were also observed in Experiment 0 N (i.e. Experiment 1B in [17]), further validating the main results. These findings suggest that force and motion are coupled as schematically shown in Fig. 1 b.

A. Force Error

In the main (5 N) experiment subjects were given visual feedback of their tangential force in two of the blocks (Fig. 2 c). In contrast to static tasks, where visual feedback enables subjects to apply a constant force quite accurately [21], the elliptic motion of the robot manipulandum in this study significantly compromised the subjects' ability to regulate force. Subjects did not eliminate residual errors, which varied periodically with motion.

Interestingly, the overall magnitude of force errors was significantly lower when the target force was lower (Fig. 4). There are several plausible explanations why this occurred. One possibility

is that greater force applied induced higher noise (i.e., signal dependent noise) [22]. Another possibility is that greater force applied induced higher hand impedance [23], which would amplify any errors between the input and actual trajectories. This would provide further support for indirect force control (Fig. 1 b).

Nonetheless, production of actual force $f(t)$ that equals input force $f_0(t)$ is possible using the indirect force control strategy of $f(t) = f_0(t) + Z\{x_0(t) - x(t)\}$ when $Z\{x_0(t) - x(t)\} = 0$ (Fig. 1 b). This can be achieved in one of two ways: (1) zero interaction dynamics and/or (2) a simultaneous prediction of the input[2] trajectory $x_0(t)$ that matches the actual trajectory $x(t)$. Thus, it is critical to note that if motion-dependent force errors were not observed, it would be impossible to distinguish between the direct and indirect force control strategies. However, the force error we observed was dominated by motion dependency (Fig. 5). Specifically, the force error was periodic with maximum auto-correlation at lag corresponding to the 180° and 360° ellipse positions (Fig. 6).

These motion-dependent force errors were also observed in both the familiarization Block F of the main experiment, where subjects were instructed to apply a constant tangential force, (Fig. 6 b) and Experiment 0 N (Fig. 6 c), where subjects were instructed to apply zero force. In both, subjects did not receive any visual feedback. Despite some practice with and without visual feedback, the motion dependency of the applied force persisted throughout the main experiment (Fig. 5). This robust observation suggests an underlying structure in humans' ability to regulate force during motion that limits the performance of this task.

B. Dynamic Primitives

Accurately controlling force would require the central nervous system to acquire an "internal model" of the task with which to "compute" predictive forward-path control inputs. The theory of dynamic primitives proposes that motor behavior, with and without physical interaction, is constructed using a limited set of primitive dynamic behaviors that are the "building blocks" of more complex actions [24]–[27]. These "building blocks" allow for a detailed plan of time-varying neuro-muscular activity to be abstracted to the parameters of a limited set of stereotyped motor patterns. Rhythmic movements can be generated by oscillations, one class of dynamic primitives. The interactive primitive is mechanical impedance. The parameters of these "building blocks" may be encoded; this may facilitate human learning, performance, and retention of complex skills.

Dynamic primitives do not preclude arbitrary patterns of force production. A sufficiently accurate internal model might be used to compute both $f_0(t)$ and the corresponding $x_0(t)$ (Fig. 1). However, if the parameters of oscillatory primitives used to plan the motion were limited, the time-course of force production would also be limited. Periodic force errors in our experimental results suggest that the controller appears to be content with "good-enough" performance, which can be obtained using a

---

[2]This input trajectory has been referred to as the zero-force trajectory, as it is the motion that would occur in the absence of external forces.

limited set of "primitive" oscillations and a sufficiently low mechanical impedance. Thus motor behavior constructed by dynamic primitives may result in performance limitations – such as the observed imperfect, periodic force regulation reported here (Fig. 5).

Other results support this account. A combination of two oscillations (e.g. in two degrees of freedom) generate the two-thirds power law relation between path curvature and angular velocity. Previous studies of crank turning suggest that during physical interaction humans generate an elliptical zero-force trajectory which exhibits a coincidence of speed and curvature extrema [28]. These observations are also consistent with the work of [17], [25], [29], [30]. The smallest force errors in [17] were observed when the velocity profile of the robot followed the two-thirds power-law relation. Moreover, position-dependent errors are evident in the results of other studies on constrained motion [31]–[33]. However, to our knowledge this is the first time that position-dependent force errors have been systematically quantified during a force regulation task with substantial motion.

C. Limitations

In the main experiment, participants experienced the task for approximately one hour (300 cycles). It is possible that participants could learn to better regulate their force with additional practice (e.g., over multiple days). However, investigation of extensive practice was not the goal of our work. Humans regularly perform a variety of novel forceful interaction tasks with ease and apparently without requiring long-term practice. In fact, task performance slightly worsened at the end of practice in the main experiment, possibly indicating that fatigue set in. Hence, this study aimed to identify the performance that might be expected from intuitive and spontaneous human-robot interaction.

Force errors might also be ascribed to poor perception of the robot's motion. However, the motion slowly ($\sim$0.33 Hz) followed a large elliptical path of 66.8 cm in circumference. Additionally, if errors in the perception of the robot's motion led to force errors, we would expect to see differences in error between the blocks that did and did not have visual feedback. Fig. 4 demonstrates that this was not observed. Motion dependent deviations from the instructed force were persistent throughout the entire main experiment (Fig. 5, & 6 a-b).

It is also possible that there may have been too much cognitive demand from mapping the vertical feedback display to the horizontal force. While this argument cannot be directly refuted from the results reported here, it is unlikely to account for our main result. Fig. 6 b shows that subjects force error was motion dependent even before visual feedback had been provided. In short, the position dependence of force error was consistent throughout the main experiment, despite the presence of visual feedback.

D. Implications

Understanding the preferred control strategy employed by humans may guide the design of robot controllers to manage physical interaction. A roboticist may draw upon the proposed "building blocks" to program a simple controller to achieve a complex task [34]–[36]. For example, a controller based on dynamic primitives has been used successfully (in simulation) to control a 2 DOF arm to manipulate a dynamically complex whip with 50 DOF in a targeting task [37]. Furthermore, the human body has a large number of redundant degrees of freedom. Kinematic redundancy has commonly been viewed as a difficult challenge to overcome, especially if control is performed via conventional optimization-based techniques. However, redundant degrees of freedom may be controlled by superposition of mechanical impedance primitives. Remarkably, unlike optimization-based methods, as the number of redundant degrees of freedom increased, control based on the superposition of impedance primitives improved; in effect, with greater redundancy control became easier [38].

The account of humans' motor control strategy proposed here may be especially useful to design controllers for robots intended to interact physically with humans. This paper demonstrated that errors in human force regulation may result from limitations in the way humans compose motor actions (e.g., possibly through dynamic primitives). These limitations should be taken into consideration in all applications involving physical human-robot interaction, including amputation prostheses, assistive exoskeletons, robot-aided rehabilitation, and physical human-robot collaboration.

VI. Conclusion

In this work, we scrutinized a pervasive assumption: force and motion can be controlled independently (an idea referred to here as direct force control). To examine this assumption, subjects were asked to apply a constant force on a robot manipulandum that moved along an elliptical path with a speed profile consistent with the preferred pattern of human motion (the two-thirds power law). Results showed that subjects were unable to control force accurately during motion, despite some practice and the presence of visual feedback; errors in force were periodic in response to the periodic motion of the robot. These results point towards an indirect force control formulation (Fig. 1 b), in which commanded motion acts through mechanical impedance to evoke force. Furthermore, the periodic pattern of path-dependent force errors was consistent with commanded motion composed of oscillatory primitives. Taken together, these findings suggest that a relatively simple mathematical model combining dynamic motion primitives with mechanical impedance, as an additional primitive, is competent to describe how humans control contact and physical interaction. A quantitative model is especially important for designing devices that physically collaborate with humans.

References

[1] G. Gulletta, W. Erlhagen, and E. Bicho, "Human-like arm motion generation: A review," *Robot. 2020*, vol. 9, vol. 9, no. 4, pp. 1–48, Dec. 2020.

[2] F. M. Campos and J. M. Calado, "Approaches to human arm movement control—A review," *Annu. Rev. Control*, vol. 33, no. 1, pp. 69–77, Apr. 2009.

[3] J.-J. E. Slotine and H. Asada, *Robot Analysis and Control*, 1st ed. New York NY, USA: Wiley., 1992.

[4] M. T. Mason, "Compliance and force control for computer controlled manipulators," *IEEE Trans. Syst. Man Cybern.*, vol. SMC-11, no. 6, pp. 418–432, 1981.

[5] M. H. Raibert and J. J. Craig, "Hybrid position/force control of manipulators," *J. Dyn. Syst. Meas. Control*, vol. 102, no. 127, pp. 126–133, 1981.

[6] V. S. Chib, M. A. Krutky, K. M. Lynch, and F. A. Mussa-Ivaldi, "The separate neural control of hand movements and contact forces," *J. Neurosci.*, vol. 29, no. 12, pp. 3939–3947, Mar. 2009.

[7] M. Casadio, A. Pressman, and F. A. Mussa-Ivaldi, "Learning to push and learning to move: The adaptive control of contact forces," *Front. Comput. Neurosci.*, vol. 9, pp. 1–17, Nov., 2015.

[8] A. P. Georgopoulos, J. Ashe, N. Smyrnis, and M. Taira, "The motor cortex and the coding of force," *Sci.*, vol. 256, no. 5064, pp. 1692–1695, Jun. 1992.

[9] C. Hamel-Pâquet, L. E. Sergio, and J. F. Kalaska, "Parietal area 5 activity does not reflect the differential time-course of motor output kinetics during arm-reaching and isometric-force tasks," *J. Neurophysiol.*, vol. 95, no. 6, pp. 3353–3370, Jun. 2006.

[10] L. E. Sergio and J. F. Kalaska, "Changes in the temporal pattern of primary motor cortex activity in a directional isometric force versus limb movement task," *J. Neurophysiol.*, vol. 80, no. 3, pp. 1577–1583, 1998.

[11] M. Kolesnikov, D. Piovesan, K. M. Lynch, and F. A. Mussa-Ivaldi, "On force regulation strategies in predictable environments," *Proc. Annu. Int. Conf. IEEE Eng. Med. Biol. Soc.*, 2011, pp. 4076–4081.

[12] D. Piovesan, M. Kolesnikov, K. Lynch, and F. A. Mussa-Ivaldi, "The concurrent control of motion and contact force in the presence of predictable disturbances," *J. Mechanisms Robot.*, vol. 11, no. 6, Dec. 2019, Art. no. 060903.

[13] E. Burdet, R. Osu, D. W. Franklin, T. E. Milner, and M. Kawato, "The central nervous system stabilizes unstable dynamics by learning optimal impedance," *Nature*, vol. 414, no. 6862, pp. 446–449, Nov. 2001.

[14] T. E. Milner and D. W. Franklin, "Impedance control and internal model use during the initial stage of adaptation to novel dynamics in humans," *J. Physiol.*, vol. 567, no. 2, pp. 651–664, Sep. 2005.

[15] R. Osu, E. Burdet, D. W. Franklin, T. E. Milner, and M. Kawato, "Different mechanisms involved in adaptation to stable and unstable dynamics," *J. Neurophysiol.*, vol. 90, no. 5, pp. 3255–3269, Nov. 2003.

[16] C. D. Takahashi, R. A. Scheidt, and D. J. Reinkensmeyer, "Impedance control and internal model formation when reaching in a randomly varying dynamical environment," *J. Neurophysiol.*, vol. 86, no. 2, pp. 1047–1051, 2001.

[17] P. Maurice, M. E. Huber, N. Hogan, and D. Sternad, "Velocity-curvature patterns limit human-robot physical interaction," *IEEE Robot. Automat. Lett.*, vol. 3, no. 1, pp. 249–256, Jan. 2018.

[18] M. Zago, A. Matic, T. Flash, A. Gomez-Marin, and F. Lacquaniti, "The speed-curvature power law of movements: A reappraisal," *Exp. Brain Res.*, vol. 236, no. 1, pp. 69–82, Jan. 2018.

[19] R. Q. Van der Linde, P. Lammertse, E. Frederiksen, and B. Ruiter, "The hapticmaster, a new high-performance haptic interface," in *Proc. Eurohaptics*. Edinburgh University, 2002, pp. 1–5.

[20] J. Kepler, *Astronomia Nova*, 1609.

[21] J. T. Massey, J. T. Lurito, G. Pellizzer, and A. P. Georgopoulos, "Three-dimensional drawings in isometric conditions: Relation between geometry and kinematics," *Exp. Brain Res.* vol. 88, no. 3, pp. 685–690, Jan.1992.

[22] R. Osu *et al.*, "Optimal impedance control for task achievement in the presence of signal-dependent noise," *J. Neuriophysiol.*, vol. 92, no. 2, pp. 1199–1215, 2004.

[23] D. B. Lipps, E. M. Baillargeon, D. Ludwig, and E. J. Perreault, "Quantifying the multidimensional impedance of the shoulder during volitional contractions," *Ann. Biomed. Eng.*, vol. 48, no. 9, pp. 2354–2369, Sep. 2020.

[24] N. Hogan and D. Sternad, "Dynamic Primitives of Motor Behavior," *Biol. Cybern.*, vol. 106, no. 11, pp. 727–739, 2012.

[25] S. Schaal and D. Sternad, "Origins and violations of the 2/3 power law in rhythmic three-dimensional arm movements," *Exp. Brain Res.*, vol. 136, no. 1, pp. 60–72, 2001.

[26] S. Schaal, "Dynamic Movement Primitives -A Framework for Motor Control in Humans and Humanoid Robotics," *Adaptive Motion Animals Machines*, pp. 261–280, Jul. 2006.

[27] S. Degallier and A. Ijspeert, "Modeling discrete and rhythmic movements through motor primitives: A review," *Biol. Cybern.*, vol. 103, no. 4, pp. 319–338, 2010.

[28] J. R. Hermus, J. Doeringer, D. Sternad, and N. Hogan, "Separating neural influences from peripheral mechanics: The speed-curvature relation in mechanically-constrained actions," *J. Neurophysiol.*, vol. 125, no. 5, pp. 1870–1885, Mar. 2020.

[29] D. Huh and T. J. Sejnowski, "Spectrum of power laws for curved hand movements," *Proc. Nat. Acad. Sci. United States Amer.*, vol. 112, no. 29, pp. E 3950–E3958, 2015.

[30] J. Hermus, D. Sternad, and N. Hogan, "Evidence for dynamic primitives in a constrained motion task," in *Proc. IEEE RAS EMBS Int. Conf. Biomed. Robot. Biomechatronics*, 2020, pp. 551–556.

[31] R. Koeppen, M.E. Huber, D. Sternad, and N. Hogan, "Controlling physical interactions: Humans do not minimize muscle effort," in *Proc. ASME Dyn. Syst. Control Conf.*, 2017, Art. no. V001T36A003.

[32] K. Ohta, M. M. Svinin, Z. Luo, S. Hosoe, and R. Laboissiére, "Optimal trajectory formation of constrained human arm reaching movements," *Biol. Cybern.*, vol. 91, no. 1, pp. 23–36, Jul. 2004.

[33] D. Russell and N. Hogan, "Dealing with constraints: A biomechanical approach," in *Proc. Images 21st Century, Proc. Annu. Int. Eng. Med. Biol. Soc.*, 1989, pp. 892–893.

[34] A. J. Ijspeert, J. Nakanishi, and S. Schaal, "Movement imitation with nonlinear dynamical systems in humanoid robots," in *Proc. IEEE Int. Conf. Robot. Automat.*, 2002, vol. 2, pp. 1398–1403.

[35] F. Stulp, E. A. Theodorou, and S. Schaal, "Reinforcement learning with sequences of motion primitives for robust manipulation," *IEEE Trans. Robot.*, vol. 28, no. 6, pp. 1360–1370, Dec. 2012.

[36] J. Peters and S. Schaal, "Policy gradient methods for robotics," in *Proc. IEEE Int. Conf. Intell. Robots Syst.*, pp. 2219–2225, 2006.

[37] M. C. Nah, A. Krotov, M. Russo, D. Sternad, and N. Hogan, "Dynamic primitives facilitate manipulating a whip," in *Proc. IEEE RAS EMBS Int. Conf. Biomed. Robot. Biomechatronics*, 2020, vol. 2020, pp. 685–691.

[38] J. Hermus, J. Lachner, D. Verdi, and N. Hogan, "Exploiting redundancy to facilitate physical interaction," *IEEE Trans. Robot.*, pp.1–17, Jul. 2021.